Progress In Electromagnetics Research, Vol. 119, 171–190, 2011

A NOVEL HIGH-POWER AMPLIFIER USING A GENERALIZED COUPLED-LINE TRANSFORMER WITH INHERENT DC-BLOCK FUNCTION

Y. Wu*, Y. Liu, S. Li, and S. Li

School of Electronic Engineering, Beijing University of Posts and Telecommunications, Beijing, China

Abstract—The purpose of this paper is to propose a novel generalized single-band transformer for two arbitrary complex load and source impedances and a novel high-power amplifier using this new transformer. By adding two reactive parts at across terminals, the coupled line with flexible electrical length has practical even- and odd-mode characteristic impedances. Thus, the total circuit layout can be realized on common printed circuit board without any restriction. The synthesis theory of this proposed transformer is complete and analytical. Furthermore, unlike conventional quarter-wavelength transformers, this structure exhibits four main features such as effective matching for extremely low-resistive load impedance, effective matching for extremely high-resistive load impedance, tunable characteristic for equivalent electrical length and inherent DC-block function. For theoretical verification, several impedance transformers, which include some fixed operating-frequency cases and a tunable case, for smaller than 7 Ohm or larger than 1500 Ohm, are presented. As a typical experimental example, this analyzed transformer with inherent DC-block function has been applied in a 4-Watt power amplifier as output matching structure.

1. INTRODUCTION

Coupled-line circuit is useful in the design of phase shifters [1] and baluns [2]. Although various kinds of amplifiers have been developed in [3–6], coupled-line circuit is not applied usually. In addition, impedance matching is a basic and important concept in microwave engineering [7, 8]. Usually, single-section (quarter-wave length) or multiple-section transmission lines (for wideband

Received 4 May 2011, Accepted 15 July 2011, Scheduled 25 July 2011

* Corresponding author: Yongle Wu (wuyongle138@gmail.com).

applications) are chosen in the design of power divider/combiner, sub-system interconnecting and power amplifiers. Furthermore, lumped-elements matching networks are also used when the operating frequency is low. For complex source and load impedances, two generalized impedance transformers [9, 10] have been proposed in 2009 to satisfy arbitrary dual-band operations. Note that these structures are still based on lossless uncoupled transmission lines. Obviously, conventional transmission lines may be unavailable as impedance transformers when the matched load impedances are extremely high, or low. This is because that the characteristic impedances of realized microstrip or other transmission lines have been limited by practical manufacturing technologies.

Recently, coupled transmission lines have been developed for impedance transformers [11–15]. Coupled-line multi-section impedance transformer in [11] performs compact circuit size. In [12], a simple configuration of coupled microstrip transmission line transformer was proposed. Unfortunately, the design methodology did not include analytical design equations, indicating optimal procedures are necessary. Then, a relatively complete design theory of coupled-line impedance transformer in [12] was presented in [13] while a wide-band transformer employing a transmission line and a coupled-line section was proposed in [14]. These two structures [13, 14] with design theory developed by Ang et al. have some same shortcomings. For examples, the mathematical solutions of design parameters are not closed-form equations and the matched load and source impedances are supposed to be real values. More important, the large coupling coefficient (for example, -5.1378 dB in the experimental transformer in [14]) is required; this increases the difficulty of microstrip realizations and limits practical applications. In addition, another kind of coupled-line impedance transformer was analyzed in [15]. Although the complex load impedances and wideband applications have been discussed in [15], the complex source impedance case and arbitrary electrical length are not included. Obviously, similar to the mathematical results of [14], the synthesis of the wideband case in [15] is complicated and the accurate circuit parameters cannot be easily obtained.

In this paper, a generalized impedance transformer for arbitrary complex source and load impedances and a novel high-power amplifier based on this transformer are proposed. By adding two flexible reactive elements and modifying electrical length of the coupled line, this coupled-line transformer not only has analytical design theory, but also makes even- and odd-mode characteristic impedances available for common microstrip fabrication technology. For verification, many kinds of numerical transformers with the theoretical results

are demonstrated. Finally, this proposed transformer is found to be an effective matching structure in the design of a high-power amplifier. From the analyzed results, we will find that the novel features of this proposed matching structure include: 1) effective matching for extremely low-resistive load impedance such as the input impedances of straight-wire dipole ($1.1–j1015\,\Omega$), normal mode helix ($4.6\,\Omega$), spherical helix ($2.2\,\Omega$) [From Table 1 in [16]], and load impedances of high-power amplifiers; 2) effective matching for extremely high-resistive load impedance (larger than $1500\,\Omega$) such as the input impedances of biconical antennas, dipole antennas, and slotline antennas with special dimensions; 3) tunable characteristic for equivalent electrical length; 4) analytical design method for arbitrary complex impedance matching; 5) inherent DC-block function. In addition, the measured results of two microstrip power amplifiers show that the proposed coupled-line impedance transformer can satisfy the requirement of the output matching network in high-power amplifier.

2. DESIGN EQUATIONS FOR THE PROPOSED COUPLED-LINE IMPEDANCE TRANSFORMER

Figure 1 shows the generalized circuit configuration of the proposed coupled-line impedance transformer. It consists of an arbitrary-length coupled line section (Z_{0e}, Z_{0o}, θ) and two reactive elements (Z_{T1}, Z_{T2}). These two reactive elements can be realized by using lumped-capacitors, lumped-inductors, lossless transmission line stubs including open-circuit case and shorted-circuit case, or a combination of reactive lumped- and distributed-elements. Five design parameters (Z_{0e}, Z_{0o}, θ, X_{T1}, X_{T2}) exist in this proposed matching structure, resulting in

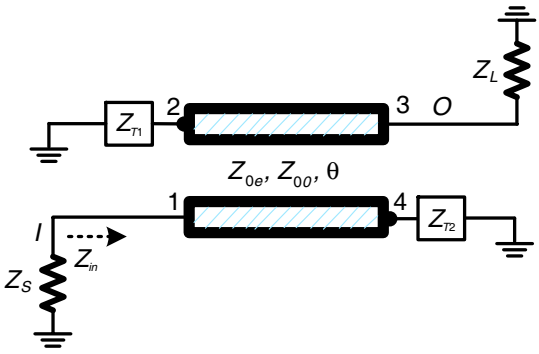

Figure 1. The circuit model of the proposed coupled-line impedance transformer.

wide range of matched source and load impedances ($Z_S = R_S + jX_S$, $Z_L = R_L + jX_L$), various available solutions, and a compact size ($\theta < 0.5\pi$).

According to the mathematical results [8], all elements of impedance matrix that describes the single arbitrary-length coupled line section with port numbers definitions, as shown in Figure 1, are symmetry. The impedance matrix elements can be expressed as

$$Z_{11} = Z_{22} = Z_{33} = Z_{44} = -j\left(\frac{Z_{0e} + Z_{0o}}{2}\right)\cot(\theta) = \frac{-jZ_a}{\tan(\theta)}, \quad (1a)$$

$$Z_{12} = Z_{21} = Z_{34} = Z_{43} = -j\left(\frac{Z_{0e} - Z_{0o}}{2}\right)\cot(\theta) = \frac{-jZ_b}{\tan(\theta)}, \quad (1b)$$

$$Z_{13} = Z_{31} = Z_{24} = Z_{42} = -j\left(\frac{Z_{0e} - Z_{0o}}{2\sin(\theta)}\right) = \frac{-jZ_b}{\sin(\theta)}, \quad (1c)$$

$$Z_{14} = Z_{41} = Z_{23} = Z_{32} = -j\left[\frac{Z_{0e} + Z_{0o}}{2\sin(\theta)}\right] = \frac{-jZ_a}{\sin(\theta)}, \quad (1d)$$

where for simplifying mathematical expression we have assumed that

$$\begin{cases} Z_a = \frac{Z_{0e}+Z_{0o}}{2}, \\ Z_b = \frac{Z_{0e}-Z_{0o}}{2}. \end{cases} \quad (2)$$

Since the values of reactive elements, Z_{T1} and Z_{T2}, are imaginary, they can be manually defined as

$$\begin{cases} Z_{T1} = jX_{T1}, \\ Z_{T2} = jX_{T2}, \end{cases} \quad (3)$$

where X_{T1} and X_{T2} must be real. It is interesting to point out that the values of both X_{T1} and X_{T2} may be zero (shorted circuit) or infinity (open circuit). They are two special cases. In addition, the values of X_{T1} can be equal or unequal to that of X_{T2}, this is determined by practical requirements.

Once the reactive elements Z_{T1} and Z_{T2} are connected to the ports 2 and 4, four-port impedance matrix can reduce to two-port impedance matrix. Here, in order to guard against confusion and misunderstanding, the ports 1 and 3 are redefined as the ports I (Input) and O (Output), as shown in Figure 1. Based on (1)–(3), the impedance matrix elements for the ports I and O are then

$$Z_{II} = j\frac{\begin{array}{c} Z_a(Z_a^2 - Z_b^2)\sin(\theta)\cos(\theta) - Z_a^2 X_{T1}\sin^2(\theta) \\ +(Z_a^2 - Z_b^2)X_{T2}\cos^2(\theta) - Z_a X_{T1} X_{T2}\sin(\theta)\cos(\theta) \end{array}}{[Z_a\cos(\theta) - X_{T2}\sin(\theta)][Z_a\cos(\theta) - X_{T1}\sin(\theta)] - Z_b^2}, \quad (4a)$$

$$Z_{IO} = Z_{OI} = j\frac{-Z_b \sin(\theta)(X_{T1}X_{T2} + Z_a^2 - Z_b^2)}{[Z_a\cos(\theta) - X_{T2}\sin(\theta)][Z_a\cos(\theta) - X_{T1}\sin(\theta)] - Z_b^2}, \quad (4b)$$

$$Z_{OO} = j\frac{\begin{array}{c} Z_a(Z_a^2 - Z_b^2)\sin(\theta)\cos(\theta) - Z_a^2 X_{T2}\sin^2(\theta) \\ +(Z_a^2 - Z_b^2)X_{T1}\cos^2(\theta) - Z_a X_{T1}X_{T2}\sin(\theta)\cos(\theta) \end{array}}{[Z_a\cos(\theta) - X_{T2}\sin(\theta)][Z_a\cos(\theta) - X_{T1}\sin(\theta)] - Z_b^2}. \quad (4c)$$

According to the conversion between the transmission ($ABCD$) matrix and the impedance matrix [8], the transmission matrix elements for the ports I and O can be obtained as

$$A = \frac{\begin{array}{c} Z_a(Z_a^2 - Z_b^2 - X_{T1}X_{T2})\sin(\theta)\cos(\theta) \\ -Z_a^2 X_{T1}\sin^2(\theta) + (Z_a^2 - Z_b^2)X_{T2}\cos^2(\theta) \end{array}}{Z_b\sin(\theta)(Z_b^2 - Z_a^2 - X_{T1}X_{T2})}, \quad (5a)$$

$$B = \frac{j}{2}\frac{\begin{array}{c} Z_a^2 X_{T1}X_{T2} + (Z_a^2 - Z_b^2)^2 - 2X_{T1}X_{T2}Z_b^2 \\ +[Z_a^2 X_{T1}X_{T2} - (Z_a^2 - Z_b^2)^2]\cos(2\theta) \\ +(X_{T1} + X_{T2})Z_a(Z_a^2 - Z_b^2)\sin(2\theta) \end{array}}{Z_b\sin(\theta)(Z_b^2 - Z_a^2 - X_{T1}X_{T2})}, \quad (5b)$$

$$C = -j\frac{[Z_a\cos(\theta) - X_{T2}\sin(\theta)][Z_a\cos(\theta) - X_{T1}\sin(\theta)] - Z_b^2}{Z_b\sin(\theta)(Z_b^2 - Z_a^2 - X_{T1}X_{T2})}, \quad (5c)$$

$$D = \frac{\begin{array}{c} Z_a(Z_a^2 - Z_b^2 - X_{T1}X_{T2})\sin(\theta)\cos(\theta) \\ -Z_a^2 X_{T2}\sin^2(\theta) + (Z_a^2 - Z_b^2)X_{T1}\cos^2(\theta) \end{array}}{Z_b\sin(\theta)(Z_b^2 - Z_a^2 - X_{T1}X_{T2})}. \quad (5d)$$

It can be observed from Figure 1 that when the perfect matching is required, the necessary situation is (The $Conj$ ( ) means conjugate operation)

$$Conj(Z_S) = \frac{AZ_L + B}{CZ_L + D}. \quad (6)$$

Substituting $Z_S = R_S + jX_S$ and $Z_L = R_L + jX_L$ into (6) and separating into real and imaginary parts gives two equations:

$$AR_L - jR_S X_L C - R_S D + jR_L X_S C = 0, \quad (7a)$$

$$B + jX_L A - R_S R_L C - X_S X_L C + jX_S D = 0. \quad (7b)$$

In Equations (7a) and (7b), the parameters R_S, R_L, X_S, X_L are known. However, other parameters such as Z_a, Z_b, θ, X_{T1}, X_{T2} are unknown and desired. Fortunately, if the values of Z_a, Z_b, θ are manually determined, other two parameters X_{T1}, X_{T2} can be calculated by closed-form equations. Both (5) and (7) are used to derive these

analytical design expressions, and the achieved results are

$$\begin{cases} X_{T1} = \frac{C_1+C_3+\sqrt{2C_2}}{C_4}, \\ X_{T2} = \frac{C_5+C_6+\sqrt{2C_2}}{C_7}, \end{cases} \tag{8a}$$

$$\begin{cases} X_{T1} = \frac{C_1+C_3-\sqrt{2C_2}}{C_4}, \\ X_{T2} = \frac{C_5+C_6-\sqrt{2C_2}}{C_7}, \end{cases} \tag{8b}$$

where

$$\begin{aligned} C_1 &= -4R_SX_LZ_a^2Z_b^2 - 2R_LX_SZ_a^2Z_b^2 + 4R_SX_LZ_b^4 \\ &\quad -R_LX_SZ_b^4 + 8R_SX_LZ_a^4\cos(2\theta) - 12R_SX_LZ_a^2Z_b^2\cos(2\theta) \\ &\quad +4R_LX_SZ_a^2Z_b^2\cos(2\theta) + 4R_SX_LZ_b^4\cos(2\theta) \\ &\quad -2R_LX_SZ_a^2Z_b^2\cos(4\theta) + R_LX_SZ_b^4\cos(4\theta), \end{aligned} \tag{9a}$$

$$\begin{aligned} C_2 &= -R_LR_S[Z_b^2 - 2Z_a^2 + Z_b^2\cos(2\theta)]^2\{8R_LR_SZ_a^4 \\ &\quad -4R_L^2R_S^2Z_b^2 - 4R_S^2X_L^2Z_b^2 - 4R_L^2X_S^2Z_b^2 - 4X_L^2X_S^2Z_b^2 \\ &\quad -16R_LR_SZ_a^2Z_b^2 - 8X_LX_SZ_a^2Z_b^2 - 4Z_a^4Z_b^2 + 11R_LR_SZ_b^4 \\ &\quad +8X_LX_SZ_b^4 + 8Z_a^2Z_b^4 - 4Z_b^6 + 4Z_b^2[R_S^2X_L^2 \\ &\quad +R_L^2(R_S^2+X_S^2) - R_LR_SZ_b^2 + (X_LX_S + Z_a^2 - Z_b^2)^2]\cos(2\theta) \\ &\quad +R_LR_SZ_b^4\cos(4\theta)\}, \end{aligned} \tag{9b}$$

$$\begin{aligned} C_3 &= -4R_L^2R_SZ_a^3\sin(2\theta) - 4R_SX_L^2Z_a^3\sin(2\theta) + 4R_SZ_a^5\sin(2\theta) \\ &\quad +4R_SZ_aR_L^2Z_b^2\sin(2\theta) - 2R_LR_S^2Z_aZ_b^2\sin(2\theta) \\ &\quad +4R_SX_L^2Z_aZ_b^2\sin(2\theta) - 2R_LX_S^2Z_aZ_b^2\sin(2\theta) \\ &\quad +2R_LZ_a^3Z_b^2\sin(2\theta) - 8R_SZ_a^3Z_b^2\sin(2\theta) - 2R_LZ_aZ_b^4\sin(2\theta) \\ &\quad +4R_SZ_aZ_b^4\sin(2\theta) + R_LR_S^2Z_aZ_b^2\sin(4\theta) \\ &\quad +R_LX_S^2Z_aZ_b^2\sin(4\theta) - R_LZ_a^3Z_b^2\sin(4\theta) + R_LZ_aZ_b^4\sin(4\theta), \end{aligned} \tag{9c}$$

$$\begin{aligned} C_4 &= -4R_L^2R_SZ_a^2 - 4X_L^2R_SZ_a^2 - 4R_SZ_a^4 + R_LR_S^2Z_b^2 \\ &\quad +R_LX_S^2Z_b^2 + 3R_LZ_a^2Z_b^2 + 8R_SZ_a^2Z_b^2 - 4R_SZ_b^4 \\ &\quad +4[R_L^2R_SZ_a^2 - R_LZ_a^2Z_b^2 + R_SX_L^2Z_a^2 - R_S(Z_a^2 - Z_b^2)^2]\cos(2\theta) \\ &\quad -R_L(R_S^2 + X_S^2 - Z_a^2)Z_b^2\cos(4\theta) + 8R_SX_LZ_a^3\sin(2\theta) \\ &\quad -8R_SX_LZ_aZ_b^2\sin(2\theta) + 4R_LX_SZ_aZ_b^2\sin(2\theta) \\ &\quad -2R_LX_SZ_aZ_b^2\sin(4\theta), \end{aligned} \tag{9d}$$

$$\begin{aligned} C_5 &= -2R_SX_LZ_a^2Z_b^2 - 4R_LX_SZ_a^2Z_b^2 + 4R_LX_SZ_b^4 - R_SX_LZ_b^4 \\ &\quad +8R_LX_SZ_a^4\cos(2\theta) - 12R_LX_SZ_a^2Z_b^2\cos(2\theta) \\ &\quad +4R_SX_LZ_a^2Z_b^2\cos(2\theta) + 4R_LX_SZ_b^4\cos(2\theta) \\ &\quad -2R_SX_LZ_a^2Z_b^2\cos(4\theta) + R_SX_LZ_b^4\cos(4\theta), \end{aligned} \tag{9e}$$

$$\begin{aligned}
C_6 \;=\; & -4R_S^2R_LZ_a^3\sin(2\theta) - 4R_LX_S^2Z_a^3\sin(2\theta) + 4R_LZ_a^5\sin(2\theta) \\
& +4R_LZ_aR_S^2Z_b^2\sin(2\theta) - 2R_SR_L^2Z_aZ_b^2\sin(2\theta) \\
& +4R_LX_S^2Z_aZ_b^2\sin(2\theta) - 2R_SX_L^2Z_aZ_b^2\sin(2\theta) \\
& +2R_SZ_a^3Z_b^2\sin(2\theta) - 8R_LZ_a^3Z_b^2\sin(2\theta) - 2R_SZ_aZ_b^4\sin(2\theta) \\
& +4R_LZ_aZ_b^4\sin(2\theta) + R_SR_L^2Z_aZ_b^2\sin(4\theta) + R_SX_L^2Z_aZ_b^2\sin(4\theta) \\
& -R_SZ_a^3Z_b^2\sin(4\theta) + R_SZ_aZ_b^4\sin(4\theta), \qquad (9f) \\
C_7 \;=\; & -4R_S^2R_LZ_a^2 - 4X_S^2R_LZ_a^2 - 4R_LZ_a^4 + R_SR_L^2Z_b^2 \\
& +R_SX_L^2Z_b^2 + 3R_SZ_a^2Z_b^2 + 8R_LZ_a^2Z_b^2 - 4R_LZ_b^4 \\
& +4[R_S^2R_LZ_a^2 - R_SZ_a^2Z_b^2 + R_LX_S^2Z_a^2 - R_L(Z_a^2 - Z_b^2)^2]\cos(2\theta) \\
& -R_S(R_L^2 + X_L^2 - Z_a^2)Z_b^2\cos(4\theta) + 8R_LX_SZ_a^3\sin(2\theta) \\
& -8R_LX_SZ_aZ_b^2\sin(2\theta) + 4R_SX_LZ_aZ_b^2\sin(2\theta) \\
& -2R_SX_LZ_aZ_b^2\sin(4\theta) \qquad (9g)
\end{aligned}$$

Equations (8a) and (8b) indicate that two solutions are possible for X_{T1} and X_{T2}. To assure these two solutions are real numbers, the argument of the square roots must be non-negative. The corresponding mathematical expression can be found as

$$C_2 \geq 0. \qquad (10)$$

Note that there are five design parameters in two Equations (7a) and (7b). This implies that the proposed coupled line transformer has three degrees of freedom. Therefore, the values of Z_a, Z_b, θ can be freely chosen when the inequality (10) is satisfied. The flexible parameter selection of Z_a and Z_b (namely, Z_{0e} and Z_{0o}) means breaking the practical limitation of microstrip coupled lines and other kinds of coupled transmission lines. Furthermore, once Z_a, Z_b, θ are known, other parameters X_{T1} and X_{T2} can be easily obtained according to (8) and (9). Since the total calculation is based on analytical formulas, the design theory of our proposed structure is direct and accurate.

3. NUMERICAL EXAMPLES OF THE PROPOSED IMPEDANCE TRANSFORMER

In this section, several numerical examples are presented to verify the above closed-form design equations including (8) and (9). As discussed above, there are many kinds of circuits available in the implementation of reactive elements X_{T1} and X_{T2}. Figure 2 illustrates five typical circuit implementation for a given reactance X_{T1} or X_{T2}. Their

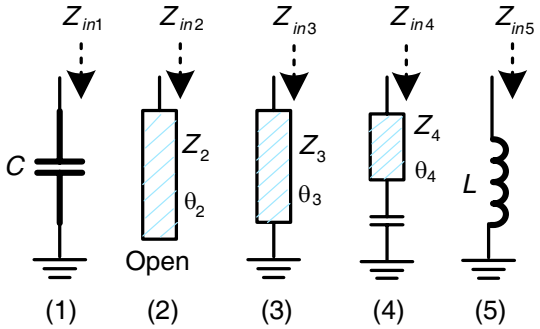

Figure 2. The typical lumped- and distributed-circuit implementation for reactive elements X_{T1} and X_{T2}.

analytical equations are obtained as

$$jX_{T1} \quad \text{or} \quad jX_{T2} = \begin{cases} Z_{in1} = j\frac{-1}{2\pi fC}, \\ Z_{in2} = j\frac{-Z_2}{\tan(\theta_2)}, \\ Z_{in3} = jZ_3\tan(\theta_3), \\ Z_{in4} = j\frac{2\pi fCZ_4^2\tan(\theta_4)-Z_4}{2\pi fCZ_4+\tan(\theta_4)}, \\ Z_{in5} = j2\pi fL. \end{cases} \tag{11}$$

Obviously, there are many kinds of other different combination structures when lossless transmission line and inductor are used simultaneously. However, generally speaking, inductors are more expensive and more difficult to realize than capacitors. Thus, the inductor (the structure (5) shown in Figure 2) is not chosen usually. Moreover, for planar transmission line such as microstrip, double-sided parallel strip line, stripline, shorted-circuit stub (the structure (3) shown in Figure 2) is harder to fabricated because a via hole is required. In summary, a pure capacitor and an open circuit stub are preferred to be utilized as the desired reactance X_{T1} or X_{T2}.

In the examples in Sections 3.1, 3.2, and 3.3, a coupled-line impedance transformer with two open circuit stubs shown in Figure 3 is considered. The characteristic impedances (Z_{T10}, Z_{T20}) of two open circuit stubs are equal to 100 Ω.

3.1. Transformers between Two Arbitrary Complex Impedances

In this section, the source and load impedances are chosen randomly as $Z_S = 50+20j\,\Omega$ and $Z_L = 10-60j\,\Omega$. The operating frequency is 2 GHz and all electrical lengths are specified at this frequency. According to

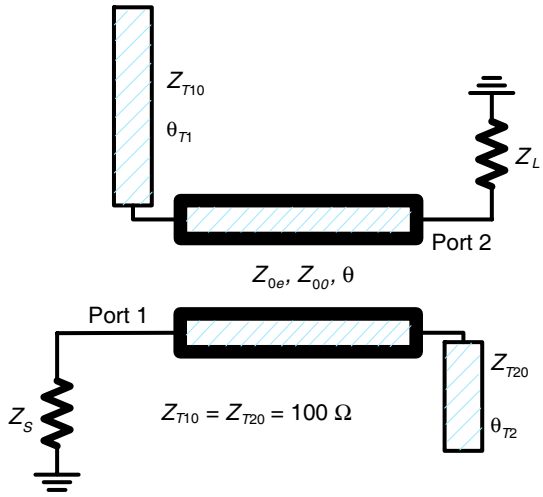

Figure 3. The typical circuit configuration of a coupled-line impedance transformer with two open circuit stubs.

Table 1. Calculated circuit parameters of the four simulated impedance transformers.

Transformers	Z_{0e} (Ω)	Z_{0o} (Ω)	θ (Degree)	θ_{T1} (Degree)	θ_{T2} (Degree)
A	110	55	60	71.4804	48.5666
B			70	64.6251	59.4780
C			80	56.5440	58.0176
D	115	62	90	42.2654	31.8065

the Equations (8b) and (11), the accurate calculated circuit parameters are obtained, as listed in Table 1, when the practical values of Z_{0e}, Z_{0o}, and θ are determined manually for microstrip. Note that the even-mode and odd-mode characteristic impedances are the same for transformers A, B, and C. But the electrical lengths are different. In addition, the transformer D presents that all parameters of the coupled line section can be adjusted freely only if (10) is satisfied. From the simulated frequency response shown in Figure 4, the ideal matching and lossless transmission at 2 GHz can be clearly observed, which verifies the proposed closed-form design formulas.

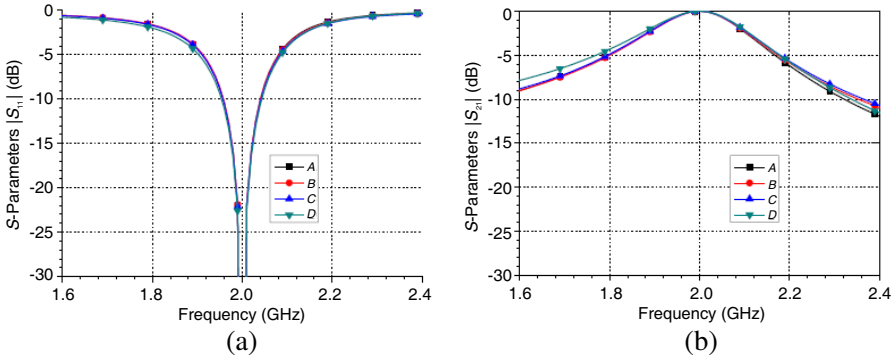

Figure 4. Frequency response of four calculated transformers (A, B, C, D) with open circuit stubs: (a) return loss and (b) insertion loss.

Table 2. Calculated circuit parameters of the impedance transformers, $E1$, $E2$, and $E3$.

Transformers	Z_L (Ω)	Z_{0e} (Ω)	Z_{0o} (Ω)	θ (Degree)	θ_{T1} (Degree)	θ_{T2} (Degree)
$E1$	7.5	110	64	60	34.9032	42.2255
$E2$	5				36.3843	58.3255
$E3$	2				36.1018	77.2193

3.2. Transformers for Matching a Extremely Low Load Impedance to a 50-Ω Standard Port

Here, the standard port impedance 50 Ω is used as the source impedance Z_S. To demonstrate the matching capability of the extremely low load impedance, three transformers with 7.5, 5, and 2 Ω load impedances are designed and the accurate circuit parameters are given in Table 2. Figure 5 shows the calculated scattering parameters when the operating frequency is 2 GHz. The electrical lengths θ_{T1} and θ_{T2} of two open circuit stubs are smaller than 90 degree, indicating that two lumped capacitors can also be used to realize the similar performance. Furthermore, the perfect matching at 2 GHz is clear in Figure 5. The return loss curves in Figure 5 also show that the bandwidth of matching decreases as the load impedance Z_L decreases.

3.3. Transformers for Matching a Extremely High Load Impedance to a 50-Ω Standard Port

Conventional quarter-wave transmission line can't be directly used to match a extremely high load impedance because the desired characteristic impedance is very large and difficult to realize. Fortunately, this proposed impedance transformer based on coupled line can overcome this difficulty. Although the transformers $F1$, $F2$, and $F3$ have larger than 1 kΩ load impedances, the final design circuit parameters listed in Table 3 are realized for traditional microstrip technology. In addition, the desired matching at the operating frequency 2 GHz is clear in the calculated return loss shown in Figure 6.

3.4. An Impedance Transformer with Tunable Operating Frequency (Electrical Length)

If the operating frequency is tunable, the equivalent electrical length should be adjusted linearly. According to this principle, four

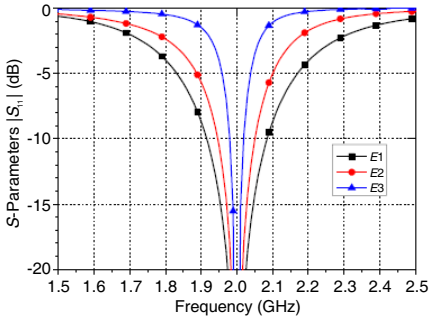

Figure 5. Frequency response (return loss) of three calculated transformers ($E1$, $E2$, and $E3$) with open circuit stubs.

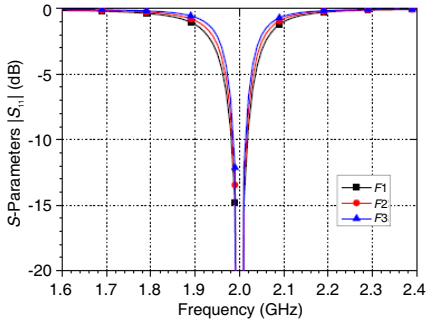

Figure 6. Frequency response (return loss) of three calculated transformers ($F1$, $F2$, and $F3$) with open circuit stubs.

Table 3. Calculated circuit parameters of the impedance transformers, $F1$, $F2$, and $F3$.

Transformers	Z_L (Ω)	Z_{0e} (Ω)	Z_{0o} (Ω)	θ (Degree)	θ_{T1} (Degree)	θ_{T2} (Degree)
$F1$	1500	100	55	80	96.1395	70.7843
$F2$	1800			70	103.4270	73.8725
$F3$	2200			60	111.2955	79.8340

impedance transformers with the same source and load impedances ($Z_S = 50\,\Omega$, $Z_L = 5\,\Omega$) are designed and their obtained parameters are listed in Table 4. Note that the operating frequencies are different. In addition, two pure capacitors are used to realize two reactive elements X_{T1} and X_{T2}. The calculated return loss presented in Figure 7 show the matching frequencies of these four transformers agree with the desired ones. From another perspective, it can be obtained from Table 4 that adjusting the values of two reactive elements X_{T1} and X_{T2} leads to a tunable operating frequency.

Table 4. Calculated circuit parameters of the impedance transformers, $G1$, $G2$, $G3$, and $G4$.

Transfor -mers	Z_{0e} (Ω)	Z_{0o} (Ω)	θ (Degree)	X_{T1}	X_{T2}
$G1$	100	55	85 (at $f =$ 1.53 GHz)	-486.3991 ($C =$ 0.2139 pF)	-91.7261 ($C =$ 1.1341 pF)
$G2$			70 (at $f =$ 1.26 GHz)	-177.8611 ($C =$ 0.7102 pF)	-61.8962 ($C =$ 2.0407 pF)
$G3$			60 (at $f =$ 1.08 GHz)	-120.0583 ($C =$ 1.2275 pF)	-52.2071 ($C =$ 2.8227 pF)
$G4$			50 (at $f =$ 0.9 GHz)	-87.0140 ($C =$ 2.0323 pF)	-51.7552 ($C =$ 3.4168 pF)

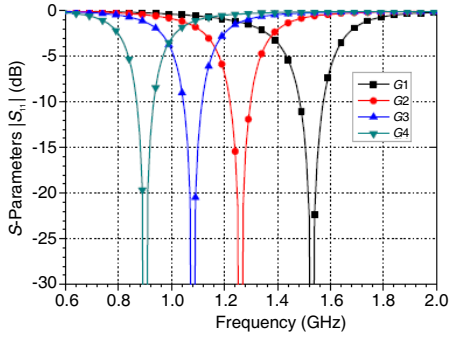

Figure 7. Frequency response (return loss) of four calculated transformers ($G1$, $G2$, $G3$, and $G4$) with two lumped capacitors.

Table 5. Calculated circuit parameters of the proposed impedance transformers.

Z_{0e} (Ω)	Z_{0o} (Ω)	θ (Degree)	θ_{T1} (Degree)	θ_{T2} (Degree)
110	65	51	33.71	14.75

In summary, it can be observed from the above examples that there are four obvious advantages in this proposed impedance transformer: 1) ideal matching performances for two arbitrary complex impedances; 2) available matching in extremely low load impedance case; 3)available matching in extremely high load impedance case; 4) flexible design for equivalent electrical length, namely, operating frequency.

4. HIGH-POWER AMPLIFIER USING THE PROPOSED IMPEDANCE TRANSFORMER

Two power amplifier modules are designed to compare the difference between the proposed impedance transformer and the traditional impedance transformer [17] in application. LDMOS Wideband Integrated Power Amplifier MW7IC2240N, which integrated on-chip input matching, DC block and Quiescent Current Temperature Compensation (QCTC), is chosen for this design. These power amplifier modules work at the frequency range from 2010 MHz to 2025 MHz which is a TD-SCDMA frequency band and the average output power level is 4 Watts.

4.1. The Design Approach

Based on the load impedance provided in the MW7IN2240N data sheet [18], the output match network should be designed to transform $5.444 + j6.869$ to $50\,\Omega$. Considering the microstrip line which is necessary for the pad of MW7IC2240N and the connection between the MW7IC2240N and the impedance transformer, the proposed impedance transformers and the traditional impedance transformer should be designed to transform $6.6 + j40.4$ to $50\,\Omega$. These calculated circuit parameters of the proposed impedance transformers are shown in Table 5. The power amplifier module which uses traditional impedance transformer (hereafter called "PA-A" for short) and the power amplifier module which uses the proposed impedance transformer (hereafter called "PA-B" for short) circuit schematics are shown in Figures 8 and 9 and the circuit component designations and

values are listed in Tables 6 and 7. The used substrate is Wangling F4BK, which has a dielectric constant of 2.65, a substrate thickness of 0.8 mm and a dissipation factor of 0.001. The size of each whole module is 145 mm × 75 mm and the layout of each amplifier is shown in Figures 10 and 11.

4.2. Measurement and Comparison

The bias point of each power amplifier is $V_{DD1} = V_{DD2} = 28\,\text{V}$, $I_{DD1} = 90\,\text{mA}$ and $I_{DD2} = 420\,\text{mA}$ (see Figures 8 and 9). Agilent N5230C PNA-L Network Analyzer is used to test the frequency response of these two power amplifier modules and the measured small-signal S-

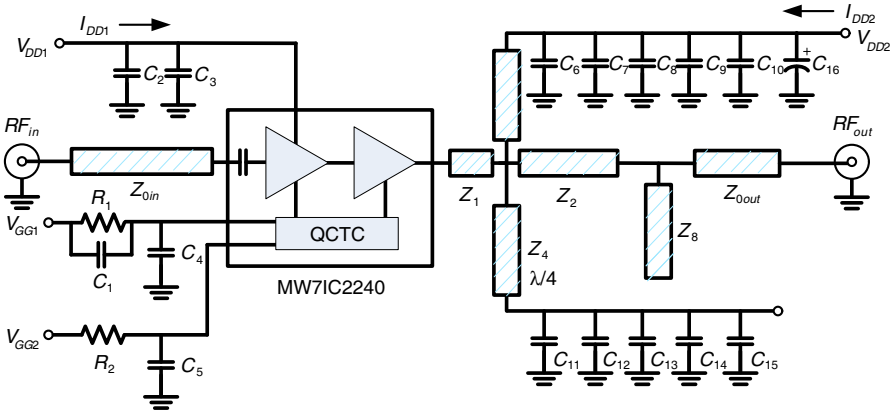

Figure 8. PA-A circuit schematic.

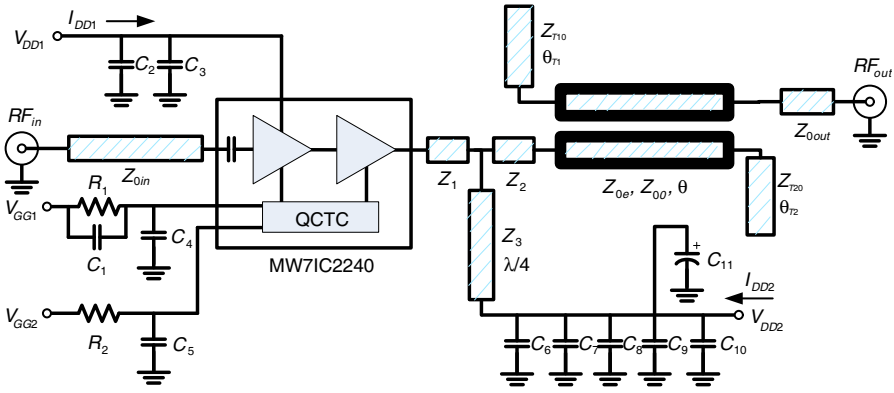

Figure 9. PA-B circuit schematic.

Table 6. PA-A circuit component designations and values.

Part	Description	Part	Description
C_1	8.2 pF Chip Capacitor	C_5, C_8, C_{13}	4.7 µF, 35 V Chip Capacitors
C_2, C_9, C_{10}, C_{14}, C_{15}	10 µF, 35 V Chip Capacitors	C_7, C_{12}	0.1 µF Chip Capacitors
C_3, C_6, C_{11}	5.6 pF Chip Capacitors	C_{16}	470 µF, 35 V Electrolytic Capacitor
C_4	0.4 pF Chip Capacitor	R_1, R_2	10 kΩ, 1/4 W Chip Resistors

Table 7. PA-B circuit component designations and values.

Part	Description	Part	Description
C_1	8.2 pF Chip Capacitor	C_5, C_8	4.7 µF, 35 V Chip Capacitors
C_2, C_9, C_{10}	10 µF, 35 V Chip Capacitors	C_7	0.1 µF Chip Capacitors
C_3, C_6	5.6 pF Chip Capacitors	C_{11}	470 µF, 35 V Electrolytic Capacitor
C_4	0.4 pF Chip Capacitor	R_1, R_2	10 kΩ, 1/4 W Chip Resistors

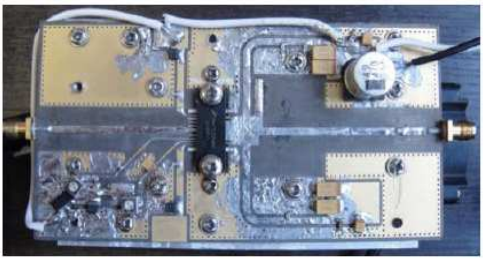

Figure 10. Photograph of the fabricated PA-A.

parameters are shown in Figures 12 and 13. As shown in Figure 12, the PA-A has 1-dB transmission bandwidth of 220 MHz and power gain of 31.8 dB. Figure 13 illustrates that the PA-B has 1-dB transmission bandwidth of 60 MHz and power gain of 34.8 dB. They indicated that PA-B has a narrower band and a higher gain. Fortunately, the

operating bandwidth of this PA-B can satisfy the requirement of base stations in the TD-SCDMA communication systems.

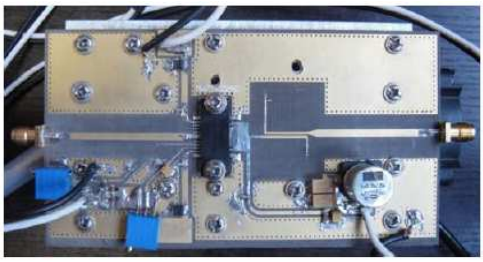

Figure 11. Photograph of the fabricated PA-B.

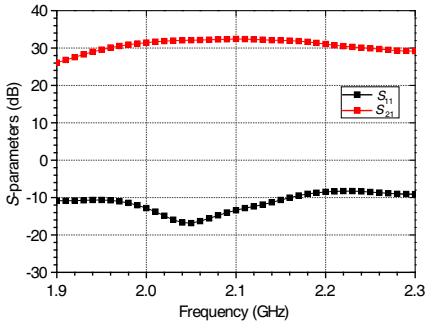

Figure 12. Frequency response of the fabricated PA-A.

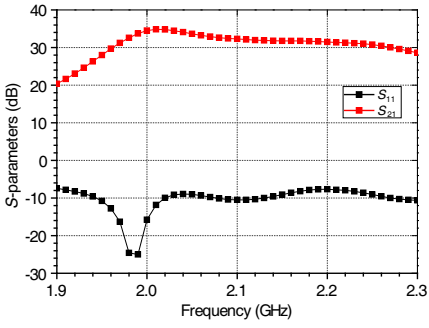

Figure 13. Frequency response of the fabricated PA-B.

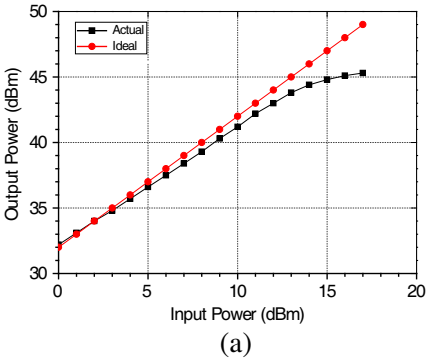

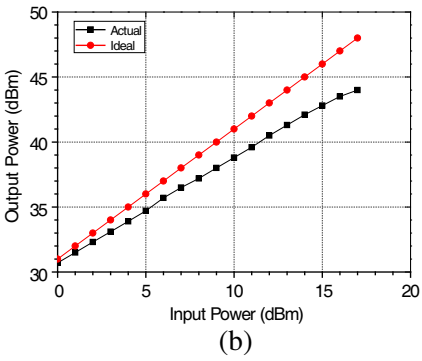

Figure 14. Pulsed CW output power versus input power: (a) PA-A, (b) PA-B.

The large-signal test system consists of Agilent E438C ESG Vector Signal Generator, Agilent N9030A PXA Signal Analyzer, and a 30 dB attenuator. The measured large-signal performance of PA-A and PA-B at 2017 MHz are illustrated in Figure 14. The linearity assessment of the designed power amplifiers were conducted by measuring the 3rd-order, 5th-order and 7th-order inter-modulation distortion (IMD) characteristics using a two-tone signal with 10-MHz tone spacing. The measured results are presented in Figures 15, 16, and 17. Figure 18 shows the measured ACPR of each power amplifier module. It can be seen that an ACPR of almost −40 dBc at 10 dB back-off has been achieved and the power amplifier module which use the proposed impedance transformer as the output match network has a better performance. Additionally, the measured maximum output power can increase to 33 Watts in the PA-B based on our proposed impedance transformer, indicating a practical high-power amplifier.

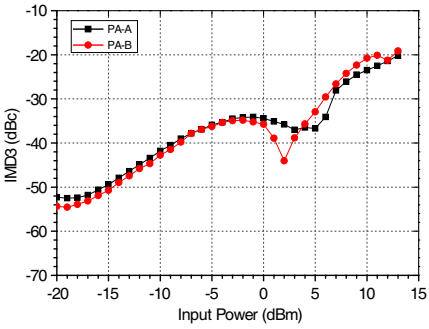

Figure 15. Measured IMD3 characteristics under two-tone signal.

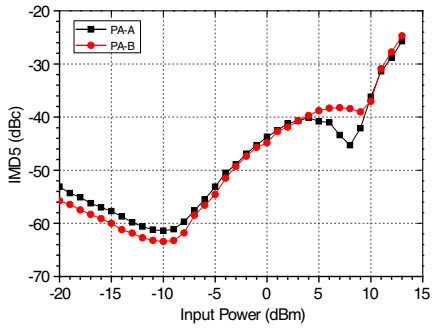

Figure 16. Measured IMD5 characteristics under two-tone signal.

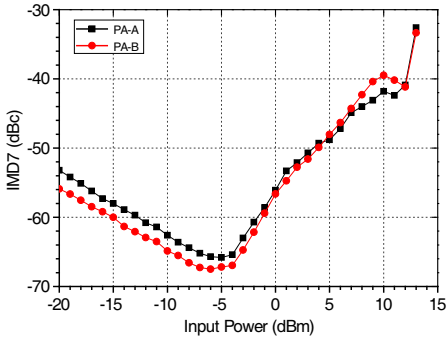

Figure 17. Measured IMD7 characteristics under two-tone signal.

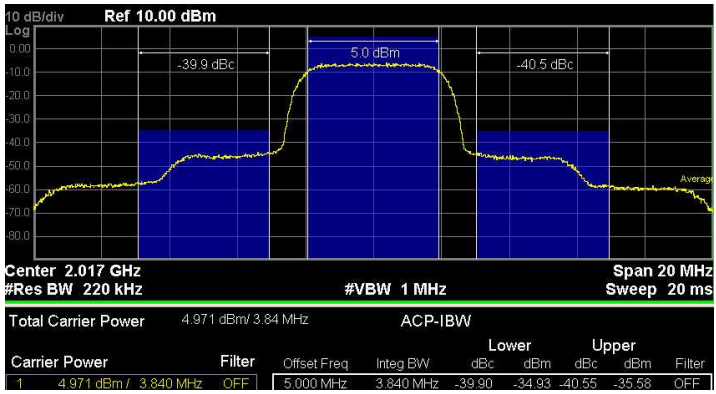

(a)

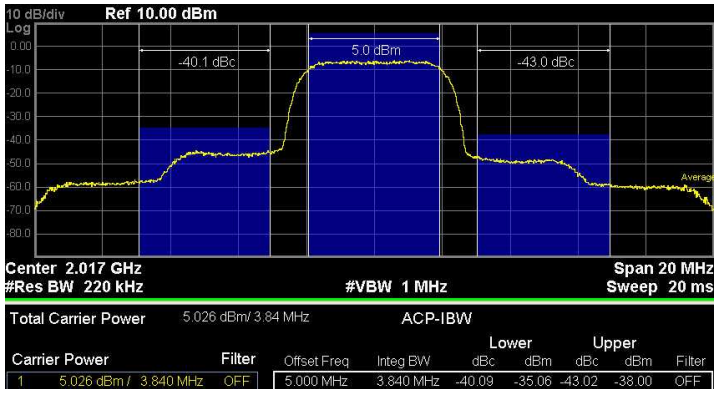

(b)

Figure 18. Measured output spectrum of (a) PA-A (b) PA-B at an average output power of 36 dBm.

5. CONCLUSION

A generalized and novel impedance transformer based on coupled line has been proposed. The corresponding closed-form design equations are given by rigorous analysis. Numerical complex impedance transformers, extremely low (or high) load impedance transformers, tunable impedance transformers are presented. Finally, a novel high-power amplifier based on this new impedance structure is designed, fabricated and demonstrated with comparable measured results. As a result, this proposed structure with analytical design approach provides another alternative matching method for the design of microwave components and systems.

ACKNOWLEDGMENT

This work was supported in part by Important National Science & Technology Specific Projects (No. 2010ZX03007-003-04), National Natural Science Foundation of China (No. 61001060). This paper is a part of Yongle Wu's doctoral dissertation.

REFERENCES

1. Gao, B. and Y. Xin, "Improved miniaturized wide-band 90-degree Schiffman phase shifter," *Journal of Electromagnetic Waves and Applications*, Vol. 23, No. 4, 493–499, 2009.
2. Jafari, E., F. Hojatkashani, and R. Rezaiesarlak, "A wideband compact planar balun for UHF DTV applications," *Journal of Electromagnetic Waves and Applications*, Vol. 23, Nos. 14–15, 2047–2053, 2009.
3. Yoon, J., H. Seo, I. Choi, and B. Kim, "Wideband LNA using a negative GM cell for improvement of linearity and noise figure," *Journal of Electromagnetic Waves and Applications*, Vol. 24, Nos. 5–6, 619–630, 2010.
4. Lee, M.-W., S.-H. Kam, Y.-S. Lee, and Y.-H. Jeong, "A highly efficient three-stage Doherty power amplifier with flat gain for WCDMA applications," *Journal of Electromagnetic Waves and Applications*, Vol. 24, Nos. 17–18, 2537–2545, 2010.
5. Zhang, B., Y.-Z. Xiong, L. Wang, S. Hu, T.-G. Lim, Y.-Q. Zhuang, and L.-W. Li, "A D-band power amplifier with 30-GHz bandwidth and 4.5-dBm P_{sat} for high-speed communication system," *Progress In Electromagnetics Research*, Vol. 107, 161–178, 2010.
6. Jimenez Martin, J. L., V. Gonzalez-Posadas, J. E. Gonzalez-Garcia, F. J. Arques-Orobon, L. E. Garcia-Munoz, and D. Segovia-Vargas, "Dual band high efficiency class ce power amplifier based on CRLH diplexer," *Progress In Electromagnetics Research*, Vol. 97, 217–240, 2009.
7. Abdalla, M. A. and Z. Hu, "Multi-band functional tunable LH impedance transformer," *Journal of Electromagnetic Waves and Applications*, Vol. 23, No. 1, 39–47, 2009.
8. Pozar, D. M., *Microwave Engineering*, 3rd edition, Nos. 2–5, 187–418, Publishing House of Electronics Industry, 2006.
9. Wu, Y., Y. Liu, and S. Li, "A dual-frequency transformer for complex impedances with two unequal sections," *IEEE Microw. Wireless Compon. Lett.*, Vol. 19, No. 2, 77–79, 2009.
10. Wu, Y., Y. Liu, S. Li, C. Yu, and X. Liu, "A generalized

dual-frequency transformer for two arbitrary complex frequency-dependent impedances," *IEEE Microw. Wireless Compon. Lett.*, Vol. 19, No. 12, 792–794, 2009.

11. Chramiec, J. and M. Kitlinski, "Design of quarter-wave compact impedance transformers using coupled transmission lines," *Electronics Letters*, Vol. 38, No. 25, 1683–1685, 2002.
12. Liu, S. P., "Planar transmission line transformer using coupled microstrip lines," *IEEE MTT-S Int. Microw. Symp. Dig.*, Vol. 2, 789–792, 1998.
13. Ang, K. S., C. H. Lee, and Y. C. Leong, "Analysis and design of coupled line impedance transformers," *IEEE MTT-S Int. Microw. Symp. Dig.*, Vol. 3, 1951–1954, 2004.
14. Ang, K. S., C. H. Lee, and Y. C. Leong, "A broad-band quarter-wavelength impedance transformer with three reflection zeros within passband," *IEEE Trans. Microw. Theory Tech.*, Vol. 52, No. 12, 2640–2644, 2004.
15. Jensen, T., V. Zhurbenko, V. Krozer, and P. Meincke, "Coupled transmission lines as impedance transformer," *IEEE Trans. Microw. Theory Tech.*, Vol. 55, No. 12, 2957–2965, 2007.
16. Best, S. R., "Low Q electrically small linear and elliptical polarized spherical dipole antennas," *IEEE Trans. Antennas Propag.*, Vol. 53, No. 3, 1047–1053, 2005.
17. Steve, C. C., *RF Power Amplifiers for Wireless Communications*, 2nd edition, No. 5, 92–100, Artech House Microwave Library, 2006.
18. Freescale Semiconductor, "RF LDMOS wideband integrated power amplifiers," Document Number: MW7IC2240N, Rev. 0, 11/2007.